

# Structural Geology of the Granite Lake Pit, Gibraltar Copper-Molybdenum Mine, South-Central British Columbia (NTS 093B/08, /09): Preliminary Observations

N. Mostaghimi, University of British Columbia, Vancouver, BC, nmostagh@eos.ubc.ca

L. Kennedy, University of British Columbia, Vancouver, BC

---

Mostaghimi, N. and Kennedy, L. (2015): Structural geology of the Granite Lake pit, Gibraltar copper-molybdenum mine, south-central British Columbia (NTS 093B/08, /09): preliminary observations; *in* Geoscience BC Summary of Activities 2014, Report 2015-1, p. 129–140.

## Introduction

The Gibraltar mine is a large calcalkaline copper-molybdenum porphyry deposit located about 10 km north of McLeese Lake, British Columbia, and hosted by tonalite of the Late Triassic Granite Mountain batholith (Figure 1). The Gibraltar deposit (MINFILE 093B 005, 006, 007, 008, 011, 012, 013; BC Geological Survey, 2014) is deformed, possessing a poorly to well-developed penetrative foliation, ductile shear zones and crosscutting brittle shear zones and faults (Ash and Riveros, 2001; Oliver, 2007a; Oliver et al., 2009; van Straaten et al., 2013). There is a known spatial association between the ore bodies and zones of ductile deformation; however, the relative timing of intrusion, mineralization and deformation has not been resolved.

This project is part of the Geological Survey of Canada's Intrusion Related Ore Systems TGI-4 program, where the Gibraltar copper-molybdenum open-pit mine is one of several mineralized systems currently being investigated. The objectives of this study are to 1) unravel the geometry and kinematics of deformation that have affected ore distribution, 2) place constraints on the timing of deformation structures and 3) determine if batholith emplacement and mineralization were synkinematic with the earliest deformation structures or if structural modification of the deposit occurred after emplacement and mineralization.

In this paper, the authors present preliminary field observations from detailed structural mapping of select benches in the Granite Lake operational pit (Figure 2).

## Regional Geological Setting

The geological setting of the Granite Mountain batholith is shown in Figure 1. The oldest rocks in the region include

---

**Keywords:** Gibraltar mine, copper-molybdenum deposit, porphyry, deformation, structural geology, Granite Mountain batholith

*This publication is also available, free of charge, as colour digital files in Adobe Acrobat® PDF format from the Geoscience BC website: <http://www.geosciencebc.com/s/DataReleases.asp>.*

late Paleozoic through early Mesozoic oceanic rocks (mainly chert, limestone and basalt) of the Cache Creek Complex (Cache Creek terrane), and Late Triassic through Middle Jurassic arc volcanic, volcanoclastic and plutonic rocks of the Quesnel terrane. Younger rocks include granitic plutons of the Middle Jurassic and Early Cretaceous, Eocene volcanic and sedimentary rocks, Oligocene–Pliocene clastic sedimentary sequences that occur along parts of the Fraser River, and widespread Miocene–Pleistocene basalt of the Chilcotin Group. Drummond et al. (1976), Tipper (1978) and Bysouth et al. (1995) thought that the Granite Mountain batholith was intrusive into the Cache Creek Complex, in part because of widespread Cache Creek exposures to the east and south of the batholith. Conversely, Ash et al. (1999a, b) and Schiarizza (2014) suggest that contacts between the batholith and the Cache Creek Complex are faults, but that intrusive contacts are preserved along the northeastern margin of the batholith where it and related plutonic rocks of the Burgess Creek stock cut an Upper Triassic volcanoclastic and volcanic sequence correlated with the Nicola Group of the Quesnel terrane. These relationships suggest that the Granite Mountain batholith is within the Quesnel terrane, and part of a panel of Quesnel terrane rocks that is faulted against the Cache Creek terrane to the west of the main Quesnel belt (Figure 1). Its age and location within the western part of Quesnel terrane suggest that the Granite Mountain batholith is broadly correlative with the Late Triassic Guichon Creek batholith, which hosts the Highland Valley copper-molybdenum porphyry deposits 250 km to the south-southeast.

## Previous Work

Early workers proposed that emplacement of the Granite Mountain batholith was syntectonic such that batholith emplacement, deformation, metamorphism and mineralization were a continuous process (Sutherland Brown, 1974; Drummond et al., 1976; Bysouth et al., 1995). Bysouth et al. (1995) presented a model where deformation of the batholith, including the formation of penetrative foliation and ductile shear zones (generally thrust faults), was related to the accretion of the Cache Creek terrane to the

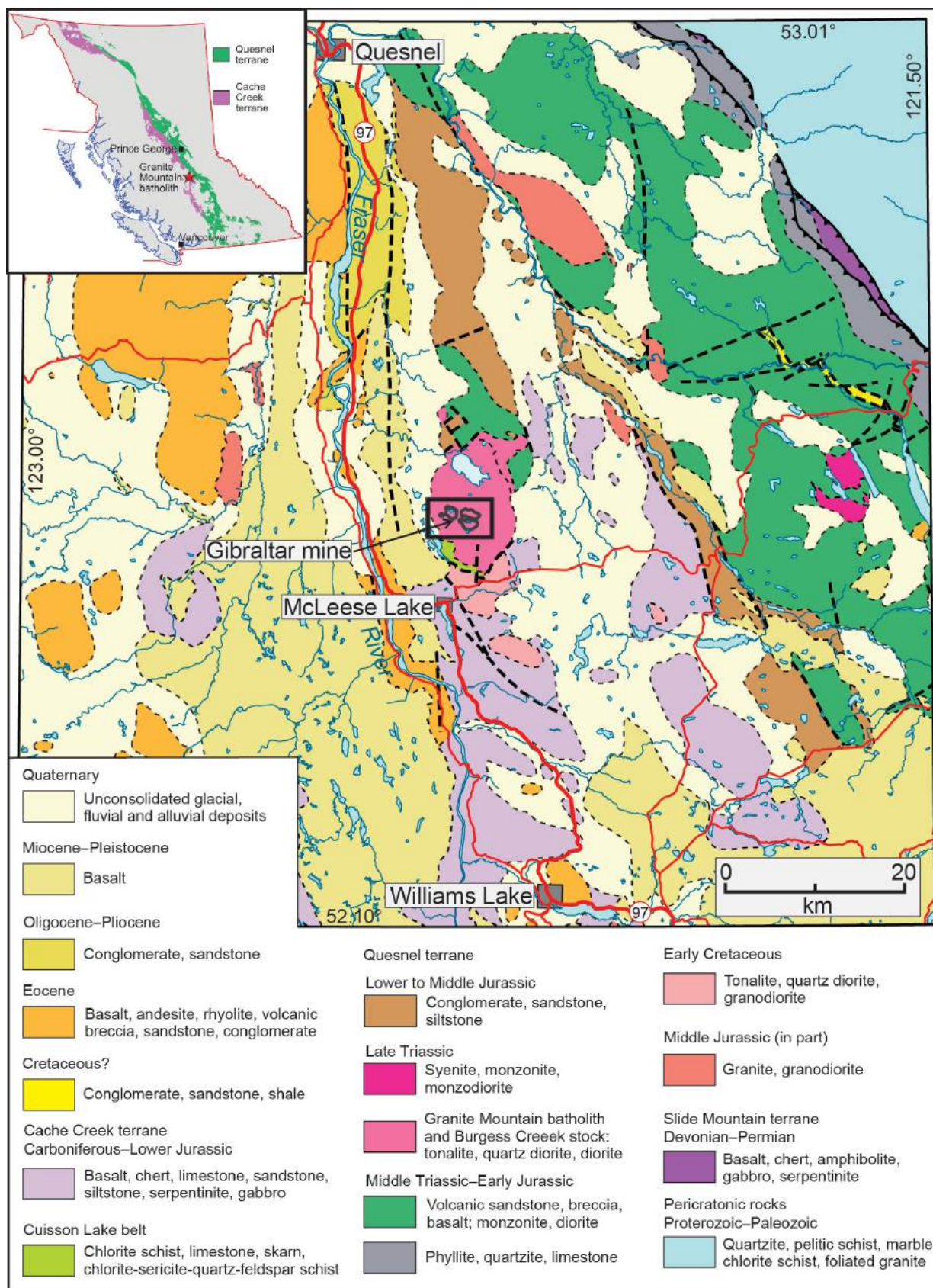


**Figure 1.** Geology of the area surrounding the Granite Mountain batholith, showing the location and setting of the Gibraltar copper-molybdenum mine (modified from Scharizza, 2014). Inset of British Columbia (top left) showing the location of the Granite Mountain batholith and the distribution of the Quesnel, Cache Creek and Slide Mountain terranes (from Scharizza, 2014).

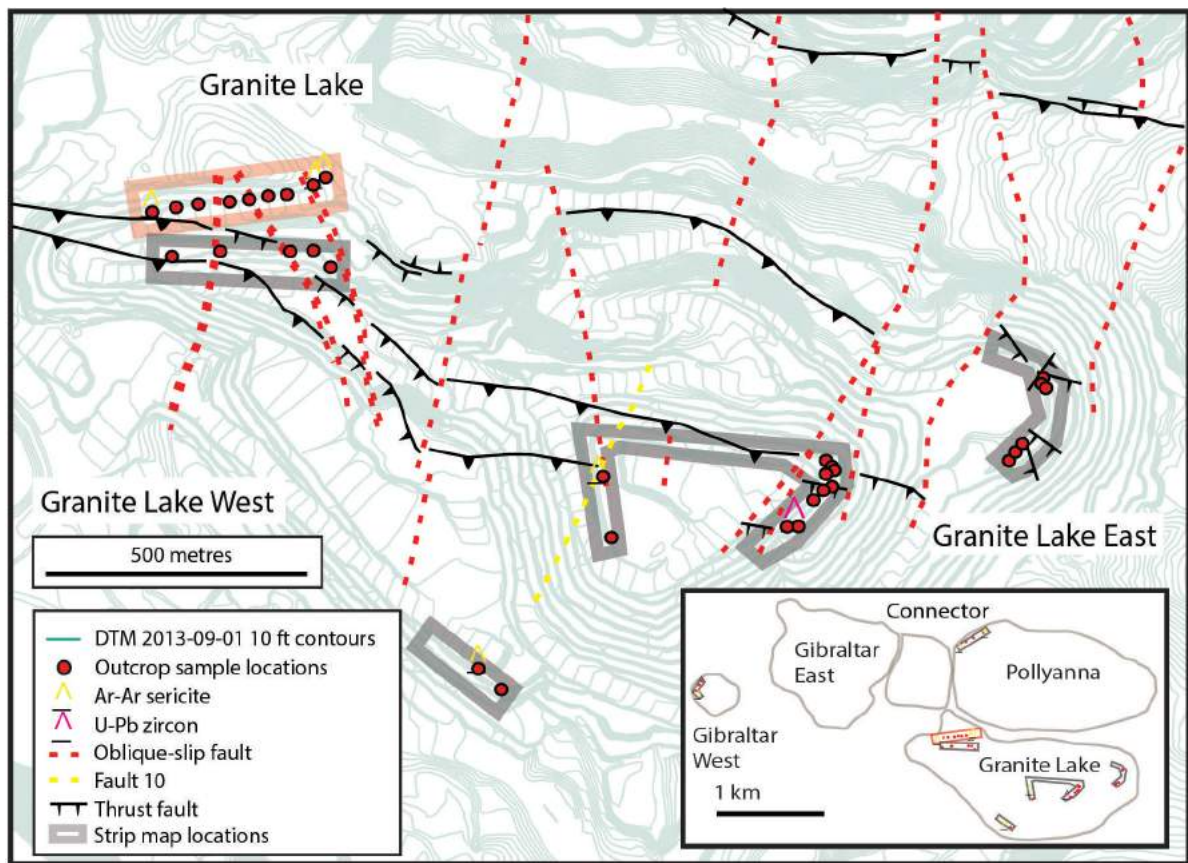


**Figure 2.** Granite Lake pit topography. Granite Lake faults offset by late north-south high-angle oblique-slip faults (dashed red lines) modified from Oliver (2008). The pit contours are from 2013, whereas the Granite Lake fault traces are from 2008 and have not been updated to the current locations where they crop out within the pit. Inset: four main pits of Gibraltar mine outlined from 2013 with the proposed Connector pit and strip map locations (modified from Jones, 2011). The strip map in Figure 3 is highlighted in red.

Quesnel terrane and was initiated before ore deposition but continued after the metals were deposited, creating the present foliated nature of the ore, alteration and hostrock (Bysouth et al., 1995). In contrast, Ash et al. (1999a, b) suggested that the ductile shear zones within the Gibraltar deposit formed during faulting of the batholith against the Cache Creek terrane, implying that either mineralization postdates intrusion or ore was remobilized into the shear zones. Late Triassic Re-Os ages on molybdenum that overlap the age of the host tonalite indicate that intrusion and mineralization are genetically linked (Harding, 2012). Van Straaten et al. (2013) argued that because ductile deformation zones contain abundant, folded, sheared and transposed hydrothermal mineralized veins, mineralization occurred either before or during deformation. The relative timing of mineralization and ductile deformation in the Gibraltar copper-molybdenum mine has not been resolved.

Deformation in the Gibraltar pits is complex because there are no true marker horizons; therefore, determining offsets and kinematics can be difficult. In general, the geometry, relative timing and kinematics of most deformation structures were documented by early workers (Sutherland

Brown, 1974; Drummond et al., 1976; Bysouth et al., 1995) and more recently by Ash et al. (1999b), Ash and Riveros (2001), Oliver et al. (2009) and van Straaten et al. (2013). The earliest tectonic fabric is a poorly to well-developed, gently to moderately southwest-dipping  $S_1$  foliation defined by chlorite and/or sericite and elongate to recrystallized quartz porphyroclasts. This foliation is best developed in proximity to high-strain zones and ranges from phyllonitic to schistose to gneissic in texture (Drummond et al., 1973; Ash and Riveros, 2001; van Straaten et al., 2013). Ash and Riveros (2001) recognized early 'sub-horizontal shear zones' that are laterally discontinuous and deform  $S_1$ . Large (tens to hundreds of metres wide), southeast- to east-trending, shallowly dipping, ductile, high-strain zones with top to the northeast sense of movement commonly host, or are spatially associated with, mineralization (e.g., Oliver, 2007a, b; Oliver et al., 2009). Oliver et al. (2009) suggest that the  $S_1$  foliation and the ductile high-strain zones formed during emplacement of the batholith and therefore exert a fundamental control on mineralization and alteration. It is likely that the formation of  $S_1$ , the subhorizontal shear zones and the ductile, compressive shear zones represent a progressive deformation. Brittle-ductile, more dis-

crete (thinner) southwest-dipping thrust faults, also with a top to the northeast shear sense are interpreted as having formed during cooling of the pluton and/or exhumation of the pluton after ductile shearing (van Straaten et al., 2013). Steeply dipping, north-striking, dextral normal fault zones offset the orebody and have similar kinematics as regional Late Cretaceous–Paleogene structures such as the Fraser, Quesnel and Pinchi fault systems.

## Ore Deposit Geology

### Lithology

The Granite Mountain batholith is subdivided into three mappable phases: Border phase quartz diorite, Mine phase tonalite and Granite Mountain phase trondhjemite (Bysouth et al., 1995). The Mine phase tonalite hosts the copper-molybdenum mineralization in the Granite Lake, Gibraltar East, Gibraltar West and Pollyanna pits (Figure 2). The Border phase quartz diorite is composed of 15% quartz, 45–50% plagioclase and 35% chloritized hornblende and is found in the southwestern segment of the batholith (van Straaten et al., 2013). The Mine phase tonalite comprises 15–25% quartz, 40–50% plagioclase and 25–35% chlorite (van Straaten et al., 2013). The rock is equigranular with grain sizes averaging 2–4 mm. Plagioclase is variably altered to albite-epidote-zoisite, and chlorite is reported to have altered from biotite and hornblende (Bysouth et al., 1995). Locally, the Mine phase tonalite contains a more leucocratic phase that contains less than 10–15% mafic minerals. The Granite Mountain phase trondhjemite to the northeast of the Mine phase tonalite comprises  $\geq 45\%$  quartz, 45% plagioclase and 10% chlorite, and is generally barren to weakly mineralized (van Straaten et al., 2013). Leucocratic quartz porphyry dikes intrude all mappable units (leucocratic phase of Bysouth et al., 1995). All phases, including the porphyry dikes, are variably deformed by  $S_1$ .

### Alteration, Veining and Mineralization

Van Straaten et al. (2013) describe vein types, alteration assemblages and mineralization distributions that are consistent with an origin as a calcalkaline porphyry. Hydrothermal alteration assemblages at the Gibraltar deposit can be used as ‘markers’ to define structures. There is a generally positive correlation between deformation intensity, alteration and mineralization (e.g., Oliver, 2007b; van Straaten et al., 2013). The vein descriptions in Table 1 provide temporal relationships between the veins and their associated alteration zone assemblages based on crosscutting relationships in the field and drillcore logging. This alteration scheme was used in the construction of the strip maps.

Hypogene mineralization, including chalcopyrite and to a lesser extent molybdenite, is predominantly vein hosted (van Straaten et al., 2013), occurring proximal to zones of

chloritization and sericitization (Bysouth et al., 1995) and is structurally controlled either during batholith emplacement or by post-emplacement modification (Drummond et al., 1973; Sutherland Brown, 1974; Bysouth et al., 1995; Ash and Riveros, 2001; Oliver et al., 2009; van Straaten et al., 2013).

## Structural Geology

Seven bench walls were mapped in Granite Lake, Pollyanna and Gibraltar West pits for lithology, alteration, structures and mineralization. A total of 50 hand samples and 30 drillcore samples were collected from selected structures and rock types for thin sections,  $^{40}\text{Ar}/^{39}\text{Ar}$  (illite) dates and U-Pb (zircon) dates (Figure 2). Below, the authors describe the structures recognized in the pits from the oldest to the youngest features; the description is focused on the Granite Lake pit and relationships are illustrated with a bench wall map from the pit (Figure 3).

The earliest fabric is a sporadically developed magmatic foliation ( $S_M$ ), defined by aligned but not strained chloritized hornblende and biotite; plagioclase is commonly saussuritized. Based on limited measurements,  $S_M$  dips gently to the northwest and southeast (Figure 4c).

The earliest tectonic fabric ( $S_1$ ) is well developed in deformation panels that are interspersed with panels of massive to poorly foliated rock. The  $S_1$  foliation is generally shallowly south dipping; however, the foliation is locally folded and poles to foliation define a weak girdle distribution (Figure 4c) with a shallowly southeast-plunging pole to the girdle. The  $S_1$  fabric is defined by elongate chloritized hornblende and elongate quartz, and ranges from weakly developed to schistose to gneissic in texture (Figures 3g, 5a–c). Increasing foliation intensity develops 1–3 mm wide subplanar chlorite ‘seams’ that are variably developed and interpreted to have formed from the accumulation, alignment and compositional zoning of chloritized primary mafic rocks. Deformation intensity is correlated with increased sericitic alteration, where  $S_1$  is defined by closely spaced sericite and chlorite lamellae. Locally, well-developed phyllonitic foliations are crenulated, with the crenulation lineations plunging shallowly to the southeast.

Early- to main-stage sheeted mineralized veins are oriented oblique and parallel to subparallel to the tectonic foliation (Figure 4; Sutherland Brown, 1974; Drummond et al., 1976; Ash and Riveros, 2001; Oliver et al., 2009) and in the field, aid in highlighting the foliation and folded foliation (Figure 5d). The sheeted veins can be folded. When present, the sheeted chlorite-epidote-quartz veins can also act as ‘C surfaces’ (in the S-C mylonite terminology): S surfaces are defined mostly by elongate quartz. This geometry gives the appearance of S-C mylonite in the field (Figure 5c) and consistently provides a top to the northeast

sense of shear. The sheeted veins clearly have slip along them, as illustrated by abundant lineated surfaces, thus, the S and C surfaces were likely kinematically linked during deformation.

It is difficult to uniquely determine if alteration and mineralization predate deformation or are syndeformational. In a weakly foliated tonalite, however, with  $S_1$  foliation defined by sericite and a weak chlorite alignment, the sericite foliation overprints previously saussuritized and veined Mine phase tonalite (Figure 5a, b). These crosscutting relationships imply that alteration and vein emplacement predate  $S_1$  formation. In highly strained rocks, foliation, veins and alteration patterns are transposed and crosscutting relationships are obliterated.

Subhorizontal, discontinuous high-strain zones (Figure 3a, b), described by Ash and Riveros (2001) as early subhorizontal shear zones, are subhorizontal to shallowly dipping toward the south-southwest and commonly contain boudinaged quartz veins with large chlorite knots and chalcopyrite±pyrite blebs (Figure 5d). Phyllonitic to schistose

$S_1$  foliation wraps around the boudinaged veins and form zones of localized high shear strain within the  $S_1$  foliation. The lineations associated with the necks of veins that are enclosed in the boudinage are shallowly plunging toward the southeast. The subhorizontal high-strain zones do not appear to be associated with any significant displacement and are interpreted to represent shearing caused by an instability related to deformation  $S_1$  fabric around the veins.

Oliver (2007a, 2008) mapped large, continuous, southeast-to east-trending, ductile, high-strain zones with reverse kinematics indicating a top to the northeast sense of movement. These high-strain zones are on the order of tens to hundreds of metres wide. In the Granite Lake pit, the high-strain zones (called Granite Lake faults; Oliver, 2007a, 2008) are bound or are spatially associated with ore mineralization (Figure 2); however, not all high-strain zones are mineralized (van Straaten et al., 2013). Drillcore intersects of these high-strain zones contain well-developed mylonite with extensive quartz grain elongation, solution transfer pressure shadows, limited dynamic recrystallization of

**Table 1.** Characteristics of the hydrothermal alteration assemblages and related vein-types at Gibraltar mine. Abbreviations: Ank, ankerite; Cb, carbonates; Chl, chlorite; Ccp, chalcopyrite; Ep, epidote; Fsp, feldspar; Hbl, hornblende; Mag, magnetite; Mol, molybdenite; Py, pyrite; Qz, quartz; QSP, quartz-sericite-pyrite; Ser, sericite; \*, data modified from van Straaten et al. (2013).

Hydrothermal alteration assemblage	Alteration characteristics	Vein assemblage	Vein shape and texture	Mineralization stage
Saussurite-chlorite (albite-epidote-zoisite)	No alteration to pale yellow-green saussuritization of feldspars, chloritized Hbl and presence of Ep veinlets	Ep	1 mm planar veinlets and 4–5 cm wide diffused flooding	Preminalization
Propylitic (chlorite-epidote)	Increase in pale yellow-green saussuritization of Fsp, chloritized Hbl, Ep grains and veinlets, and Chl-Ep veins*	Chl+Ep±Py±Cpy±Qz±Cb	1–15 mm wide Chl-Ep vein: a) thin, planar; b) wider, diffuse margins; c) wider, diffuse Qz envelope; d) Cb and cubic Py in the centre ±Ccp	Early
Chlorite-quartz	Alteration intensity characterized by vein density and ranges from no pervasive matrix alteration to prevalent Qz and Chl replacement of Fsp*	Qz±Chl±Mag±Py±Ccp±Mol	2–20 mm wide Qz vein with Chl halo; sometimes Mag-Chl-Mol-Ccp±Py aligned in centre: a) sharp boundaries; b) no margins, grey Qz; and c) disconnected, wavy veins with more diffuse Qz-Chl margins*	Main
Quartz-sericite	Qz-Ser flooding	Qz+Ser	Qz-Ser flooding and replacement of Chl-Qz-Fsp alteration	Late
Quartz-sericite-chlorite	Finely disseminated Ser±pale Chl±Qz alteration of matrix; euhedral grains of Py are sparse	~	No specific vein is closely associated with this alteration	Late
Phyllic (quartz-sericite-pyrite)	Occurs in varying intensities; weak QSP alteration is distinguished by 1–3 cm wide sheeted veins, while stronger QSP alteration is characterized by pervasive replacement of the matrix by Qz and Ser*	Qtz+Ser+Py±Ccp±Mol	a) 1–3 cm wide sheeted grey Qz veins, with Ser-Qz envelopes and cubic Py aligned in the centre; b) 1–200 cm wide milky-white veins, with parallel sheeted Mo veinlets, host bulk Mo mineralization (Harding, 2012)	Late
Ankerite-quartz	Pale Ank-Qz alteration commonly associated with high strain zones; sulphide mineralization may occur with Ser±Chl folia*	Ank whisps	2 mm in size, separated sinuous whisps; veins were either completely deformed or transposed as they are unidentifiable	Late
~	Not associated with any specific alteration assemblage	Qtz+Chl±Ccp±Py±Cb	0.1–1 m thick, boudinaged Qz veins with Chl knots ±Py±Ccp blebs, enveloped by Chl/Ser folia	Late or postmineralization

Granite Lake West:  
3770' - 3850'  
Ramp

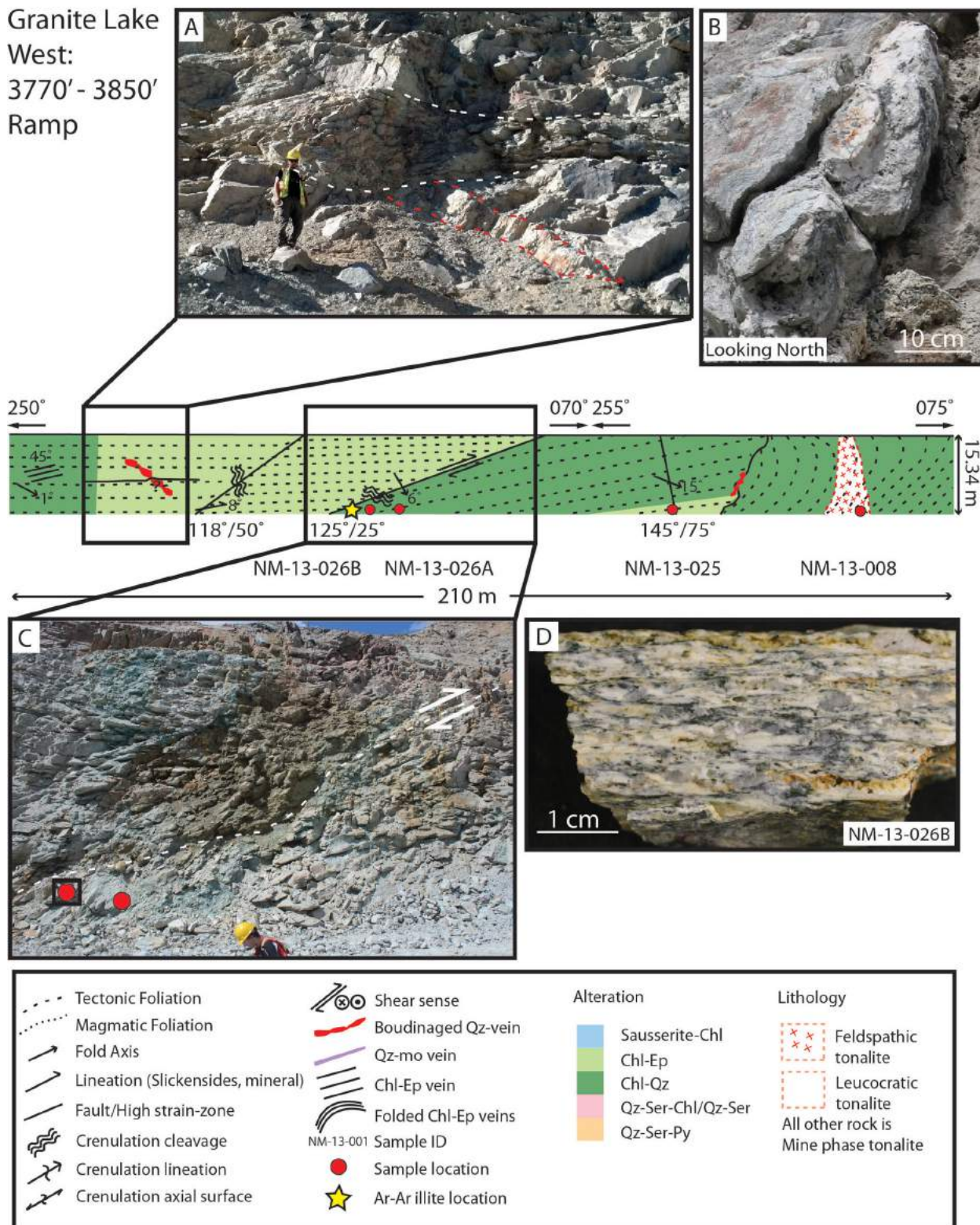


**Figure 3.** Bench-wall geological strip map from Granite Lake West, coloured according to the predominant (>50%) alteration assemblage. Figure 3a is the western end of the exposure; Figure 3e is the eastern end of the bench. Foliation intensity increases with decreasing space between form (strike) lines: **a**) subhorizontal, discontinuous, high-strain zone (outlined by white dashed lines) oblique to a boudinaged quartz vein; **b**) boudinaged quartz vein located in a high-angle fault from a different bench wall in Granite Lake West pit; similar boudinaged quartz veins are observed in subhorizontal discontinuous high-strain zones; lineations defined by the boudin neck plunging shallowly toward the southeast; **c**) imbricate thrust fault with a distributed zone of strain and a narrow (~30 cm thick) mylonitic fault core; **d**) sample from the core of the thrust fault, showing mylonitic fabric with fault zone-parallel chlorite layers and elongate quartz; sample collected from the red dot in the box of c).

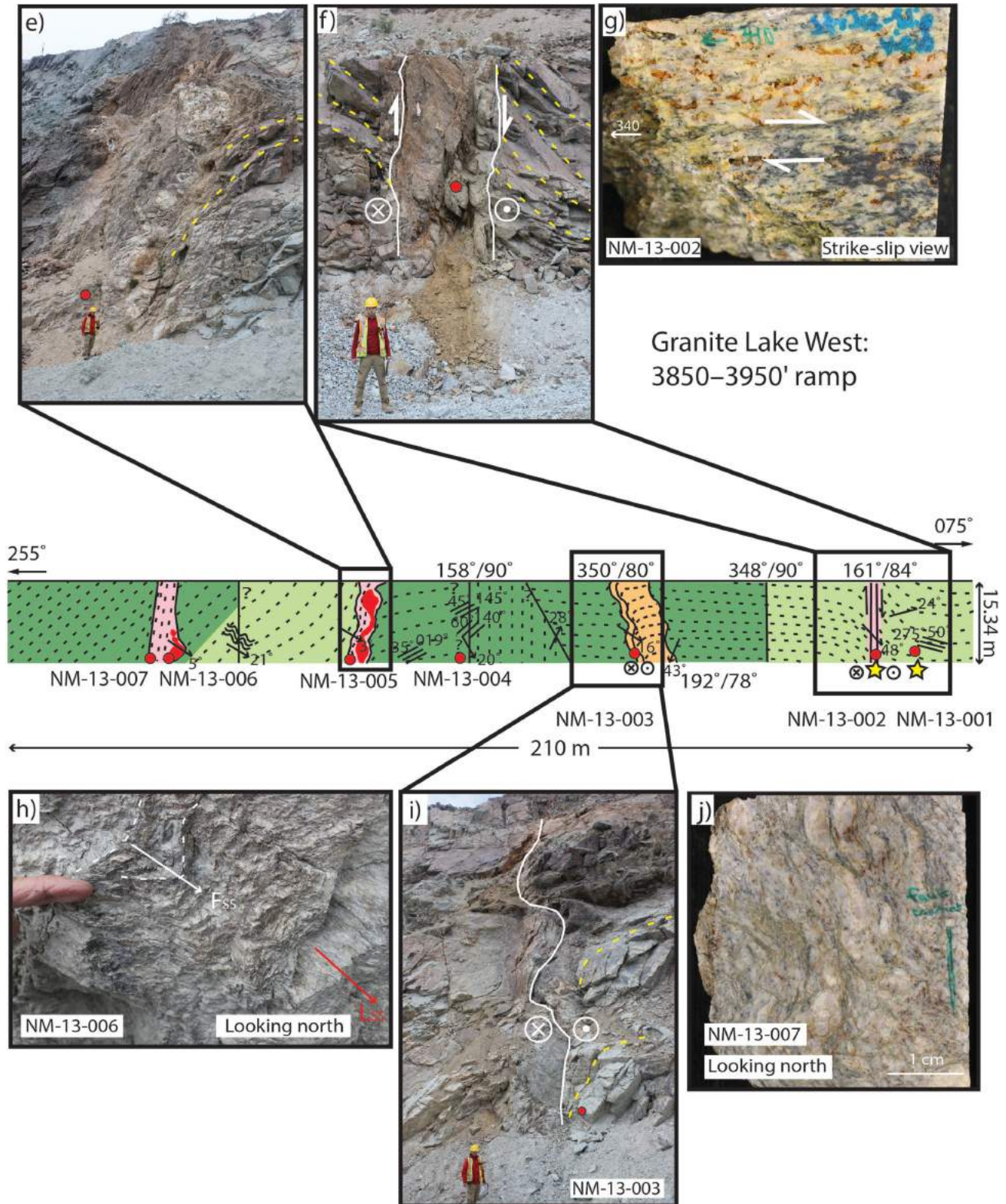


**Figure 3 (continued).** **e)** high-angle oblique-slip fault with boudinaged quartz-rich vein, boudins are elongated parallel to fault strike; **f)** high-angle dextral-normal fault zone;  $S_1$  foliation is dragged into the fault; **g)** dextral shear sense shown by the asymmetry of quartz pressure shadows; sample collected from the red dot in **f)**; **h)** parallel fold axes ( $F_{SS}$ ) and muscovite lineations ( $L_{SS}$ ) plunging 5° toward 130°; sample collected from a high-angle fault; **i)** folded dextral, high-angle fault zone; fold axes plunge shallowly toward the southeast; **j)** highly strained fault rock with a crenulated fault fabric; sample taken from a high-angle oblique-slip fault.

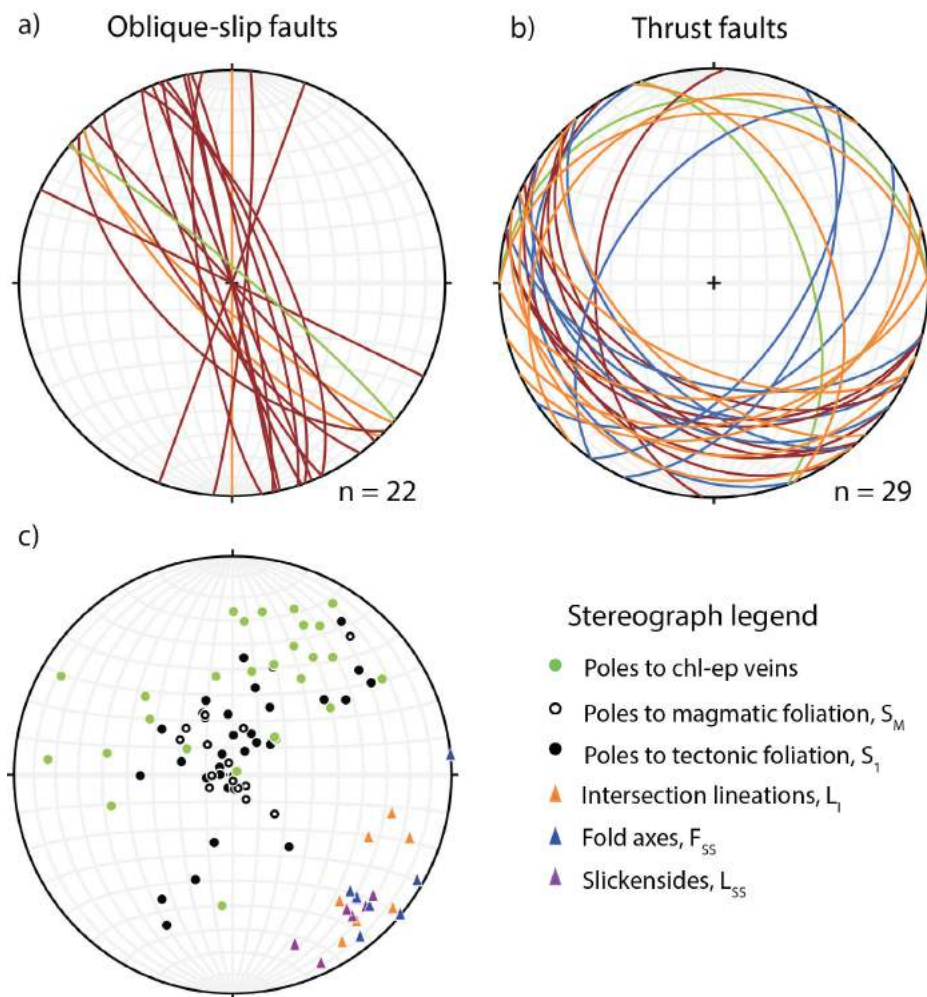


**Figure 4.** **a)** Stereographs of high-angle dextral-normal fault planes from Granite Lake West (in red), Pollyanna (in orange) and Gibraltar West (in green); **b)** stereographs of thrust faults, same colour scheme as in a) and Granite Lake East is in blue; **c)** stereograph of structural elements from the Granite Lake pit; poles to early mineralization-stage chlorite-epidote veins,  $n = 27$ ; poles to magmatic foliation,  $n = 20$ ; poles to tectonic foliation,  $n = 32$ ; intersection lineations between  $S_1$  and oblique-slip fault fabric ( $L_1$ ),  $n = 10$ ; fold axes within high-angle, oblique-slip faults ( $F_{SS}$ ),  $n = 9$ ; and slickensides and mineral lineations within high-angle, oblique-slip faults ( $L_{SS}$ ),  $n = 6$ .

quartz (Figure 5e, f) and higher degrees of alteration than less strained rock, suggesting that fluid flow assisted deformation. In the high-strain zones, veins are folded, sheared and transposed parallel to the main fabric. Large quartz clasts observed in mylonite are probably sheared and fragmented veins.

Smaller-scale thrust faults (Figure 3c) with the same attitude and shear sense as the Granite Lake faults are common in the Granite Lake, Pollyanna and Gibraltar West pits. They strike  $110\text{--}150^\circ$  and dip  $20\text{--}55^\circ$  toward the south-southwest (Figure 4b). These thrusts are imbricate in their spatial geometry, are more discrete than the larger Granite Lake faults and contain mylonitic zones up to 30 cm thick (Figure 3c, d). The presence of mylonite rather than brittle fault rocks implies that the physical conditions of deformation (e.g., temperature) were similar during the formation of both the Granite Lake faults and the imbricate thrust

faults. The imbricate thrusts are typically associated with high concentrations of copper oxides. In addition, boudinaged quartz veins enriched in chalcopyrite±pyrite are found within the thrust faults, indicating the remobilization of ore during thrust fault formation. Drag folds of  $S_1$  into the thrust faults provide reliable shear sense indicators and indicate that  $S_1$  existed prior to thrusting. Northeast-dipping thrust faults, with little to no mylonite developed, are spatially associated with the southwest-dipping thrusts, and are interpreted as conjugate faults. The strongly foliated rocks found in the Granite Lake faults, and in the more localized imbricate thrust faults, are crenulated (Figures 3h, 5f). The crenulation and intersection lineations plunge shallowly to the southeast.

The imbricate thrust faults offset and stack the ore body (Oliver, 2007a). Van Straaten et al. (2013) interpret the imbricate thrust faults as having formed during cooling and/or

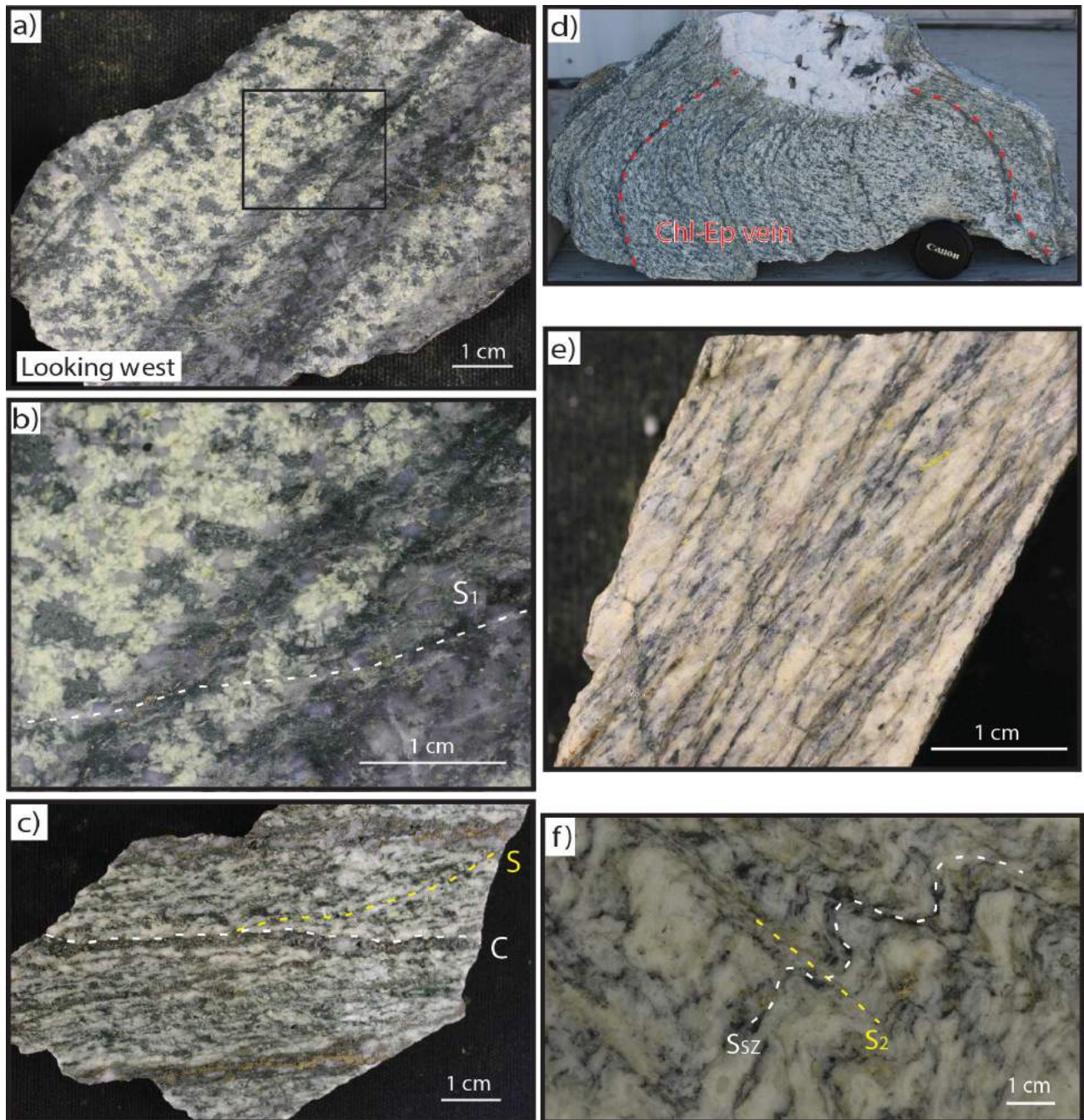


**Figure 5.** a) Mineralized chlorite-epidote-quartz-chalcopryrite vein overprinted by a weak  $S_1$  foliation defined by sericite and elongate quartz;  $S_1$  changes orientation from shallow in the chlorite-epidote-altered tonalite to more inclined in the vein due to rheological differences between the background rock and the vein; sample collected from Granite Lake East; box showing location of b); b) inset of a) illustrating the  $S_1$  foliation crosscutting the chlorite-epidote-quartz-chalcopryrite vein; c) S-C fabric in chlorite-quartz-altered Mine phase tonalite; the C surface is defined by mineralized chlorite-epidote-quartz-chalcopryrite veins, the S surface is defined by elongate quartz and inclined chlorite seams; sample collected from Granite Lake West; d) boudinaged late- or postmineralization-stage quartz vein with chlorite knots; dashed red lines highlight the folded mineralized chlorite-epidote-quartz-chalcopryrite veins in chlorite-epidote-altered Mine phase tonalite; sample collected from Granite Lake East; e) drillcore sample of a weakly mineralized ankerite-quartz-altered high-strain zone from a Granite Lake fault; f) drillcore sample of weakly mineralized, ankerite-quartz-altered leucocratic tonalite, with shear zone foliation ( $S_{sz}$ ) cut by  $S_2$  crenulation cleavage; sample taken from a Granite Lake fault.

exhumation after the ductile shearing. The authors of this paper suggest that large, ductile, high-strain zones and the imbricate thrust faults are kinematically linked during the same phase of deformation.

High-angle, oblique-slip fault zones strike northwest to northeast, are steeply dipping and crosscut all units and structures (Figure 4a; Oliver et al., 2009). Drag folds of  $S_1$  indicate a component of normal shear (Figure 3f) and shear-sense indicators from cataclasite (observed from the strike-slip kinematic plane) indicate dextral shear sense (Figure 3g). These fault zones have damage zones up to 5 m wide, and the fault zone cores have foliated cataclasite that can be up to 1 m thick. The foliation within the cataclasite is defined mostly by layers of quartz and illite (Figure 3g). Well-developed mineral lineations (illite and elongate quartz) and slickenlines plunge shallowly toward the southeast (Figures 3h, j, 4c). Folds are common in the fault zones and fold axes trend shallowly to the southeast (Figure 3h). Fault fabrics from all observed high-angle dextral-normal faults are crenulated, the intersection lineation and crenulation lineations plunge shallowly to the southeast (Figure 4c). The high-angle faults can be folded (Figure 3i) with fold axes subparallel to crenulation lineations (Figure 3h). When present in the high-angle dextral faults, late leucocratic dikes and thick, late quartz veins are folded and boudinaged (Figure 3e). Late-stage quartz-sericite-pyrite-molybdenite veins are tightly folded in these faults.

Large, brittle faults with thick gouge zones appear to be the latest brittle deformation feature. In the Granite Lake pit, these faults are exemplified by Fault 10 (Figure 2), which strikes  $200^\circ$ , dips  $44^\circ$  to the west and is marked by a 20 m thick zone of hematite staining Fault 10. Although the displacement is not known, this fault and others like it (or smaller in size) are generally geotechnical hazards causing slumping or pit wall failures within the pits.

## Conclusions

The authors propose that the formation of  $S_1$ , the formation of the subhorizontal high-strain zones, the large, ductile, compressive high-strain zones and the smaller scale thrust faults are all part of a progressive deformation that occurred under the same directed stress. Mineralized sheeted veins that occur parallel to subparallel to  $S_1$  act as pre-existing C surfaces and locally facilitate the formation of S-C mylonite. Subhorizontal, discontinuous high-strain zones are not well understood; however, they are interpreted to be caused by instabilities arising from the flattening of foliation around large veins. North-striking oblique-slip faults contain brittle fault rocks (foliated cataclasite) that suggest their formation in upper levels of the crust. These faults likely formed at higher levels in the crust than the main foliation and associated high-strain zones. Exhumation and uplift of the Granite Mountain batholith may be related to slip

along the oblique-slip faults and/or the late brittle faults. The shallowly southeast-plunging lineations, including intersections, fold axes and boudin necks, must represent the last stage deformation: the cause of this late-stage flattening resulting in boudinage and crenulations is not yet resolved.

## Future Work

Several cross sections of the Granite Lake pit will be constructed based on field observations, logged drillcore and fault offset information gleaned from using Leapfrog® Geo visualization with all drillcore data from Granite Lake. The main foliation ( $S_1$ ) and the different shear zones will be dated using Ar-Ar (illite) from fabrics with known kinematics. The Mine phase tonalite will be dated using U-Pb (zircon). Microstructural observations will allow constraints to be placed on the physical conditions (e.g., temperature) of deformation for each deformation structure. Ultimately, the goal is to constrain the absolute age of deformation and to determine the relative timing of intrusion, mineralization and deformation.

## Acknowledgments

The authors are grateful to Taseko Mines Ltd. for allowing access to the pits, the drillcore and their database. The authors thank L. Goodman for her assistance with the database and for assistance in the field. B. van Straaten is thanked for sharing his knowledge regarding the alteration and for beneficial discussions. Natural Resources Canada provided partial funding for this project. N. Mostaghimi is thankful for the generous financial support provided by Geoscience BC. The authors thank P. Schiarizza for his careful review of the manuscript.

## References

- Ash, C.H. and Riveros, C.P. (2001): Geology of the Gibraltar copper molybdenite deposit, east-central British Columbia (93B/9); *in* Geological Fieldwork 2000, BC Ministry of Energy and Mines, BC Geological Survey, Paper 2001-1, p. 119–133.
- Ash, C.H., Rydman, M.O., Payne, C.W. and Panteleyev, A. (1999a): Geological setting of the Gibraltar mine, south-central British Columbia (93B/8, 9); *in* Exploration and Mining in British Columbia 1998, BC Ministry of Energy and Mines, BC Geological Survey, p. A1–A15.
- Ash, C.H., Panteleyev, A., MacLennan, K.L., Payne, C.W. and Rydman, M.O. (1999b): Geology of the Gibraltar mine area, NTS 93B/8, 9; BC Ministry of Energy and Mines, BC Geological Survey, Open File 1999-7, scale 1:50 000.
- BC Geological Survey (2014): MINFILE BC mineral deposits database; BC Ministry of Energy and Mines, URL <<http://minfile.ca>> [November 2014].
- Bysouth, G.D., Campbell, K.V., Barker, G.E. and Gagnier, G.K. (1995): Tonalite-trondhjemite fractionation of peraluminous magma and the formation of syntectonic porphyry copper mineralization, Gibraltar mine, central British Co-

- lumbia; *in* Porphyry Deposits of the Northwestern Cordillera of North America, T.G. Schroeter (ed.), Canadian Institute of Mining and Metallurgy, v. 46, p. 201–213.
- Drummond, A.D., Tennant, S.J. and Young, R.J. (1973): The interrelationship of regional metamorphism, hydrothermal alteration and mineralization at the Gibraltar Mines copper deposit in B.C.; Canadian Institute of Mining, Metallurgy and Petroleum, Bulletin, v. 66, p. 48–55.
- Drummond, A.D., Sutherland Brown, A., Young, R.J. and Tennant, S.J. (1976): Gibraltar – regional metamorphism, mineralization, hydrothermal alteration and structural development; *in* Porphyry Deposits of the Canadian Cordillera, A. Sutherland Brown (ed.), Canadian Institute of Mining and Metallurgy, Special Volume 15, p. 195–205.
- Harding, B. (2012): The characterization of molybdenum mineralization at the Gibraltar mines Cu-Mo porphyry, central British Columbia; B.Sc. thesis, Queen’s University, 52 p.
- Jones, S. (2011): Technical report on the 357 million ton increase in mineral reserves at the Gibraltar mine, British Columbia, Canada: NI 43-101 report by Taseko Mines Limited; URL <<http://www.sedar.com/>> [November 2014]
- Oliver, J. (2007a): Pollyanna – Granite Lake geological and structural domains; unpublished internal report for Gibraltar Mines, 8 p.
- Oliver, J. (2007b): Gibraltar mines GIB East pit field trip transect; unpublished internal report for Gibraltar Mines, 14 p.
- Oliver, J. (2008): Geological map of Granite Lake pit; unpublished internal map for Gibraltar Mines.
- Oliver, J., Crozier, J., Kamionko, M. and Fleming, J. (2009): The Gibraltar mine, British Columbia. A billion tonne deep copper-molybdenum porphyry system: structural style, patterns of mineralization and rock alteration; *in* Association for Mineral Exploration British Columbia, 2009 Mineral Exploration Roundup, program with abstracts, p. 35–36.
- Schiarizza, P. (2014): Geological setting of the Granite Mountain batholith, host to the Gibraltar porphyry Cu-Mo deposit, south-central British Columbia; *in* Geological Fieldwork 2013, British Columbia Ministry of Energy and Mines, British Columbia Geological Survey, Paper 2014-1, p. 95–110, URL <[http://www.empr.gov.bc.ca/Mining/Geoscience/PublicationsCatalogue/Fieldwork/Documents/2013/06\\_Schiarizza.pdf](http://www.empr.gov.bc.ca/Mining/Geoscience/PublicationsCatalogue/Fieldwork/Documents/2013/06_Schiarizza.pdf)> [November 2014]
- Sutherland Brown, A. (1974): Gibraltar mine (93B-12, 13); *in* Geology, Exploration and Mining in British Columbia 1973, BC Ministry of Energy and Mines, BC Geological Survey, p. 299–318.
- Tipper, H.W. (1978): Northeastern part of Quesnel (93B) map-area, British Columbia; *in* Current Research, Part A, Geological Survey of Canada, Paper 78-1A, p. 67–68.
- van Straaten, B.I., Oliver, J., Crozier, J. and Goodhue, L. (2013): A summary of the Gibraltar porphyry copper-molybdenum deposit, south-central British Columbia, Canada; *in* Porphyry systems of central and southern BC: Prince George to Princeton, J. Logan and T. G. Schroeter (ed.), Society of Economic Geologists Field Trip Guidebook, v. 43, p. 55–66.

